ChemPubSoc Europe

DOI: 10.1002/cphc.201402615

Structural and Magnetic Properties of $CoGe_n^-$ ($n=2$–11) Clusters: Photoelectron Spectroscopy and Density Functional Calculations

Xiao-Jiao Deng, Xiang-Yu Kong, Xi-Ling Xu, Hong-Guang Xu,* and Wei-Jun Zheng*[a]

A series of cobalt-doped germanium clusters, $CoGe_n^{-/0}$ ($n=2$–11), are investigated by using anion photoelectron spectroscopy combined with density functional theory calculations. For both anionic and neutral $CoGe_n$ ($n=2$–11) clusters, the critical size of the transition from exo- to endohedral structures is $n=9$. Natural population analysis shows that there is electron transfer from the Ge_n framework to the Co atom at $n=7$–11 for both anionic and neutral $CoGe_n$ clusters. The magnetic moments of the anionic and neutral $CoGe_n$ clusters decrease to the lowest values at $n=10$ and 11. The transfer of electrons from the Ge_n framework to the Co atom and the minimization of the magnetic moments are related to the evolution of $CoGe_n$ structures from exo- to endohedral.

1. Introduction

Germanium clusters have attracted much attention because germanium has high carrier mobility and has potential applications in high-speed electronics.[1,2] Metal-doped germanium clusters have also been investigated by theoretical calculations and are believed to have potential applications in many fields.[3–26] Unlike carbon atoms, germanium atoms prefer to interact with each other through sp^3 hybridization; thus, pure germanium clusters are not able to form cage structures. Some theoretical and experimental studies suggested that the doping of transition metals (TMs) could improve the stabilization of the cage structures of germanium-based clusters and tailor their properties at the same time.[8,11,27–29] Moreover, stable TM-doped germanium clusters may be used as building blocks for cluster-assembled materials.[4,5,30]

It has been reported that cobalt-doped germanium nanomaterials have low resistivity, high thermal stability, and room temperature ferromagnetism; this results in potential applications in effective on-chip interconnects and nanoelectrodes for highly integrated nanoelectronic devices, spintronic devices, and field-emission displays.[31–36] Investigating the structural and electronic properties of cobalt-doped germanium clusters may provide valuable information for developing cobalt/germanium materials, as well as their applications in electronic and magnetic materials. There have been several experimental and theoretical studies on cobalt-doped germanium clusters. Zhang et al. generated Co–Ge clusters by laser vaporization and observed a relatively strong $CoGe_{10}^-$ signal in the mass spectrum.[27] Li et al. investigated the structure of $CoGe_{10}^-$ through density functional theory (DFT) calculations and suggested that the most stable structure of $CoGe_{10}^-$ was a D_{4d} bicapped tetragonal antiprism and the second most stable structure was a C_{3v} tetracapped trigonal prism.[3] Subsequently, the $CoGe_{10}^{3-}$ cluster anion was synthesized and cocrystallized with the anion $[Co(C_8H_{12})_2]^-$ in the compound $[K(2,2,2\text{-crypt})]_4[Co@Ge_{10}]$–$[Co(C_8H_{12})_2]\cdot$toluene (2,2,2-crypt = 4,7,13,16,21,24-hexaoxa-1,10-diazabicyclo[8.8.8]hexacosane), and single-crystal X-ray structural characterization suggested that $CoGe_{10}^{3-}$ exhibited a D_{5d} pentagonal prismatic structure.[37] The structural and magnetic properties of $CoGe_n$ ($n=1$–13) clusters were also investigated by Jing et al.[12] and Kapila et al.[19] through DFT calculations. Recently, Uta et al. conducted a DFT study on $Co@Ge_{10}^z$ with charges ranging from -5 to $+1$, and predicted a singlet C_{3v} polyhedral structure for $Co@Ge_{10}^-$ and a singlet pentagonal prismatic structure for $Co@Ge_{10}^{3-}$.[25] Compared with the number of theoretical studies, there have been very few experimental studies. Regarding the electronic properties of cobalt-doped germanium clusters, there is no experimental data available.

Because photoelectron spectroscopy is a very useful and straightforward technique for exploring the electronic structures of clusters, herein, we investigated $CoGe_n^-$ ($n=2$–11) clusters by using mass-selected anion photoelectron spectroscopy experiments combined with DFT calculations to provide more detailed information about the structural and electronic properties of $CoGe_n$ clusters.

2. Results and Discussion

2.1. Experimental Results

The photoelectron spectra of $CoGe_n^-$ ($n=2$–11) clusters taken with $\lambda=266$ nm (4.661 eV) photons are plotted in Figure 1.

[a] X.-J. Deng, Dr. X.-Y. Kong, Dr. X.-L. Xu, Dr. H.-G. Xu, Prof. Dr. W.-J. Zheng
State Key Laboratory of Molecular Reaction Dynamics
Institute of Chemistry, Chinese Academy of Sciences
Beijing 100190 (P.R. China)
E-mail: xuhong@iccas.ac.cn
zhengwj@iccas.ac.cn

Supporting Information for this article is available on the WWW under http://dx.doi.org/10.1002/cphc.201402615.

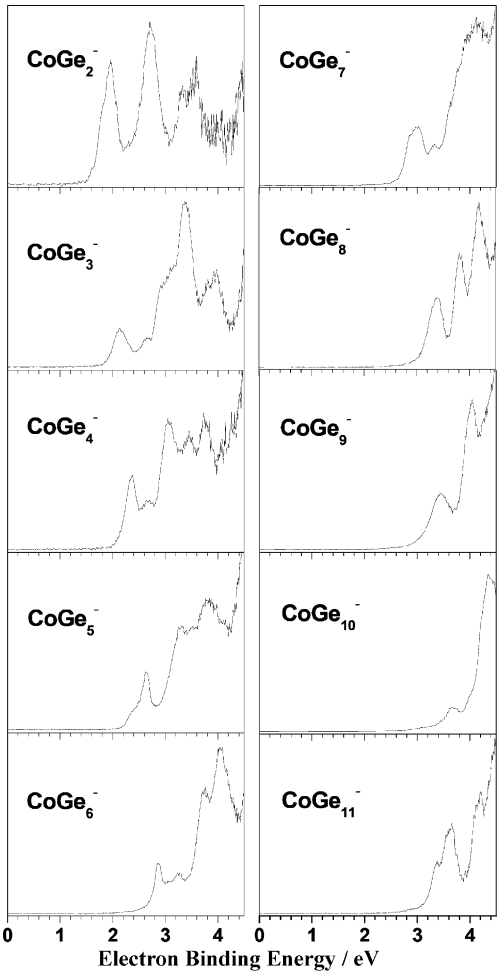

Figure 1. Photoelectron spectra of $CoGe_n^-$ ($n=2$–11) clusters recorded with $\lambda=266$ nm photons.

The vertical detachment energies (VDEs) and adiabatic detachment energies (ADEs) of these clusters obtained from the photoelectron spectra are listed in Table 1. The VDEs were estimated from the maxima of the first peaks. The ADEs were determined by drawing a straight line along the leading edge of the first peaks to cross the baseline of the spectra and adding the instrument resolution to the electron binding energy (EBE) values at the crossing points.

Table 1. Experimentally observed VDEs and ADEs from the photoelectron spectra of $CoGe_n^-$ ($n=2$–11) clusters.

Cluster	VDE [eV]	ADE [eV]
$CoGe_2^-$	1.96 ± 0.08	1.56 ± 0.08
$CoGe_3^-$	2.12 ± 0.08	1.85 ± 0.08
$CoGe_4^-$	2.38 ± 0.08	2.10 ± 0.08
$CoGe_5^-$	2.64 ± 0.08	2.42 ± 0.08
$CoGe_6^-$	2.86 ± 0.08	2.71 ± 0.08
$CoGe_7^-$	2.84 ± 0.08	2.65 ± 0.08
$CoGe_8^-$	3.39 ± 0.08	3.05 ± 0.08
$CoGe_9^-$	3.44 ± 0.08	3.00 ± 0.08
$CoGe_{10}^-$	3.63 ± 0.08	2.78 ± 0.08
$CoGe_{11}^-$	3.38 ± 0.08	3.11 ± 0.08

The spectrum of $CoGe_2^-$ shows two resolved peaks centered at 1.96 and 2.71 eV, and two barely resolved peaks centered at 3.33 and 3.60 eV, respectively. As for the spectrum of $CoGe_3^-$, there are two relatively weaker peaks centered at 2.12 and 2.66 eV, and two large peaks at 3.37 and 3.98 eV, respectively. There is also a shoulder at about 3.00 eV. The spectrum of $CoGe_4^-$ exhibits at least five peaks centered at 2.38, 2.63, 3.06, 3.45, and 3.74 eV. With respect to $CoGe_5^-$, it has a peak centered at 2.64 eV and a small shoulder at the low binding energy side, followed by three unresolved broad peaks at 3.25, 3.77, and above 4.0 eV. In the spectrum of $CoGe_6^-$, there are two small peaks centered at 2.86 and 3.23 eV, and two large peaks centered at 3.77 and 4.03 eV. The spectrum of $CoGe_7^-$ has three peaks centered at 2.84, 3.32, and 4.11 eV. In the spectrum of $CoGe_8^-$, there are three discernible peaks centered at 3.39, 3.80, and 4.18 eV; the first peak has a small shoulder at 3.06 eV. There are two distinguishable peaks centered at 3.44 and 4.05 eV and an additional one beyond 4.2 eV in the spectrum of $CoGe_9^-$. The spectrum of $CoGe_{10}^-$ displays two resolved peaks centered at 3.63 and 4.33 eV, respectively. For the spectrum of $CoGe_{11}^-$, four barely resolved peaks centered at 3.38, 3.65, 4.19 eV, and above 4.4 eV can be observed.

2.2. Theoretical Results

The typical low-lying isomers of $CoGe_n^-$ ($n=2$–11) clusters obtained from DFT calculations are presented in Figure 2, with the most stable ones on the left. The relative energies of these isomers, as well as their theoretical VDEs and ADEs, are summarized in Table 2. The Cartesian coordinates of these isomers are available in the Supporting Information, SI.

2.2.1. $CoGe_2^-$

The most stable isomer of $CoGe_2^-$ cluster (2A; Figure 2) is a triangle with C_{2v} symmetry. Isomer 2B has a structure similar to that of 2A, but with different spin multiplicities, and it is 0.83 eV higher in energy than 2A (Table 2). The linear structure (2C) with the cobalt atom located at one end is much less stable in energy than isomer 2A by 1.04 eV, and its calculated VDE (2.50 eV) is much higher than the experimental value (1.96 eV). The theoretical VDE of isomer 2A (1.86 eV) is in good agreement with the experimental value. Therefore, we suggest that isomer 2A is the most probable structure detected in our experiments.

2.2.2. $CoGe_3^-$

For the $CoGe_3^-$ cluster, the lowest energy isomer, 3A (Figure 2), is a planar rhombus. The theoretical VDE of isomer 3A (2.30 eV; Table 2) is consistent with the experimental value (2.12 eV). The tetrahedral (3B) and bent rhombus (3C) structures are higher in energy than 3A by 0.45 and 0.60 eV, respectively. The existence of isomers 3B and 3C in the experiments can be ruled out because they are much less stable. Thus, isomer 3A is the most probable isomer observed in our experiments.

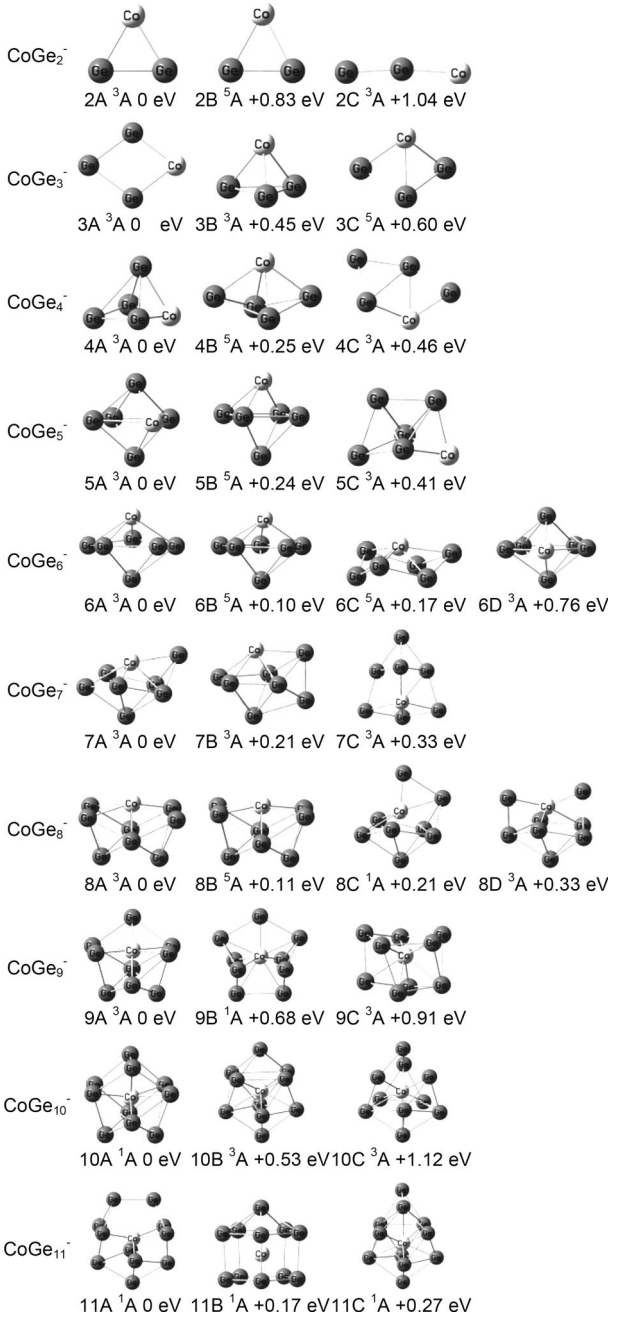

Figure 2. Optimized geometries of the low-lying isomers of $CoGe_n^-$ ($n=2$–11) clusters. The relative energies to the most stable isomers are shown.

2.2.3. $CoGe_4^-$

The most stable isomer of the $CoGe_4^-$ cluster (4A; Figure 2) can be seen as a distorted square pyramid with the cobalt atom at the square base. Isomer 4B is a triangular bipyramid, and it is 0.25 eV less stable than 4A in energy. Isomer 4C can be described as a Ge atom interacting with one edge of a bent $CoGe_3$ rhombus. The calculated VDEs (2.37, 2.21, and 2.33 eV ; Table 2) of these isomers are close to the experimental value (2.38 eV), but the energy of isomer 4C is higher than that of 4A by 0.46 eV. Therefore, the existence of isomer 4C in the experiments can be excluded. We suggest that isomer 4A is the major isomer detected in our experiments and isomer 4B may exist with low abundance.

Table 2. Relative energies of the low-energy isomers of $CoGe_n^-$ ($n=2$–11) clusters, as well as their VDEs and ADEs obtained by DFT calculations.

Isomer		Symmetry	State	ΔE [eV]	VDE [eV]		ADE [eV]	
					Theor	Exptl	Theor	Exptl
$CoGe_2^-$	**2A**	C_{2v}	^3A	0	1.86	1.96	1.85	1.56
	2B	C_s	^5A	0.83	1.12		1.02	
	2C	C_s	^3A	1.04	2.50		2.46	
$CoGe_3^-$	**3A**	C_{2v}	^3A	0	2.30	2.12	2.21	1.85
	3B	C_{3v}	^3A	0.45	1.92		1.86	
	3C	C_s	^5A	0.60	2.09		1.71	
$CoGe_4^-$	**4A**	C_s	^3A	0	2.37	2.38	2.22	2.10
	4B	C_{2v}	^5A	0.25	2.21		2.00	
	4C	C_1	^3A	0.46	2.33		1.93	
$CoGe_5^-$	**5A**	C_2	^3A	0	2.96	2.64	2.44	2.42
	5B	C_{4v}	^5A	0.24	2.55		2.28	
	5C	C_s	^3A	0.41	2.58		2.03	
$CoGe_6^-$	**6A**	C_s	^3A	0	2.83	2.86	2.64	2.71
	6B	C_1	^5A	0.10	2.97		2.48	
	6C	C_{3v}	^5A	0.17	3.19		3.09	
	6D	C_{2v}	^3A	0.76	2.28		1.92	
$CoGe_7^-$	**7A**	C_s	^3A	0	2.72	2.84	2.67	2.65
	7B	C_1	^3A	0.21	2.98		2.81	
	7C	C_s	^3A	0.33	3.08		2.82	
$CoGe_8^-$	**8A**	C_s	^3A	0	3.09	3.39	2.92	3.05
	8B	C_{2v}	^5A	0.11	2.99		2.83	
	8C	C_1	^1A	0.21	3.30		2.76	
	8D	C_1	^3A	0.33	3.15		2.78	
$CoGe_9^-$	**9A**	C_{3v}	^3A	0	3.27	3.44	3.16	3.00
	9B	C_{2v}	^1A	0.68	3.83		2.97	
	9C	C_1	^3A	0.91	3.27		2.26	
$CoGe_{10}^-$	**10A**	C_1	^1A	0	3.35	3.63	3.15	2.78
	10B	C_1	^3A	0.53	2.89		2.63	
	10C	C_1	^3A	1.12	3.00		2.03	
$CoGe_{11}^-$	**11A**	C_{2v}	^1A	0	3.27	3.38	3.18	3.11
	11B	C_1	^1A	0.17	3.18		3.09	
	11C	C_s	^1A	0.27	3.00		2.80	

2.2.4. $CoGe_5^-$

For the $CoGe_5^-$ cluster, isomers 5A and 5B (Figure 2) are square bipyramids with the cobalt atom at the square base and vertex, respectively, and 5B is higher in energy than 5A by 0.24 eV. The VDE of isomer 5A is calculated to be 2.96 eV, close to the broad peaks near 3.0 eV in the experimental spectrum of $CoGe_5^-$ (Table 2). The calculated VDE of isomer 5B is 2.55 eV, close to the first peak at 2.64 eV and the small shoulder in the experimental spectrum. Isomer 5C is higher in energy than 5A by 0.41 eV. Its existence in the experiments can be ruled out. We suggest that isomers 5A and 5B are the most probable ones detected in the experiments.

2.2.5. $CoGe_6^-$

For the $CoGe_6^-$ cluster, isomers 6A and 6B (Figure 2) are pentagonal bipyramids with the cobalt atom at the vertex with different spin multiplicities, and 6B is only 0.10 eV higher in energy than 6A. Isomer 6B can be considered as a low-lying electronic excited state of isomer 6A. Isomer 6C can be de-

scribed as the cobalt atom located on top of the Ge_6 chair-shaped framework, and it is higher in energy than 6A by 0.17 eV. Isomer 6D is also a pentagonal bipyramid, but with the cobalt atom at the equatorial ring. The theoretical VDEs of isomers 6A and 6B (2.83 and 2.97 eV; Table 2) are in good agreement with the experimental value (2.86 eV). The calculated VDE of 6C is 3.19 eV, which is very close to the second peak in the experimental spectrum. The calculated VDE of 6D (2.28 eV) is much lower than the experimental value. We suggest that isomers 6A and 6B are the most probable structures observed in our experiments, but the existence of 6C cannot be ruled out.

2.2.6. $CoGe_7^-$

The lowest-lying isomer of $CoGe_7^-$ cluster (7A; Figure 2) can be seen as a germanium atom capping a distorted pentagonal bipyramid. Isomer 7B can be described as two germanium atoms capping two faces of a $CoGe_5$ square bipyramid. The calculated VDE of isomer 7A (2.72 eV; Table 2) is in good agreement with the experimental value (2.84 eV). Isomer 7A is the most probable isomer detected in our experiment, but the existence of 7B cannot be ruled out because it is higher in energy than isomer 7A by only 0.21 eV and its calculated VDE (2.98 eV) is also close to the experimental VDE. The existence of isomer 7C in the experiments can be ruled out because it is higher in energy than 7A by 0.33 eV.

2.2.7. $CoGe_8^-$

For the $CoGe_8^-$ cluster, the most stable isomer (8A; Figure 2) can be considered as a half-endohedral structure with the cobalt atom sitting in a boat-shaped Ge_8 framework. Isomer 8A can also be viewed as two square bipyramids sharing one face. The same structure was named a tricapped-trigonal prism by Jing et al.[12] and Kapila et al.[19] Isomer 8B has a structure similar to 8A, but with different spin multiplicities, and it can be considered as a low-lying electronic excited state of isomer 8A. Isomer 8C can be viewed as a germanium atom capping a distorted $CoGe_6$ pentagonal bipyramid and another germanium atom interacting with the cobalt atom on the top. The theoretical VDEs of 8A and 8B are 3.09 and 2.99 eV, respectively (Table 2), which are lower than the VDE of the first feature in the experimental spectrum, but close to the shoulder at 3.06 eV and the front part of the first feature. The theoretical VDE (3.30 eV) of isomer 8C is in good agreement with the experimental value, and it is only 0.21 eV higher in energy than isomer 8A. The existence of isomer 8D in the experiments can be ruled out because it is higher in energy than 8A by 0.33 eV. Therefore, we suggest that isomers 8A, 8B, and 8C coexist in our experiments.

2.2.8. $CoGe_9^-$

With respect to the $CoGe_9^-$ cluster, the lowest energy isomer (9A; Figure 2) can be described as a germanium atom capping the boat-shaped structure of $CoGe_8^-$ (isomer 8A). Therefore, it is one step further toward the formation of a fully endohedral structure. The theoretical VDE (3.27 eV) is very close to the experimental value (3.44 eV; Table 2). Isomers 9B and 9C are much higher than 9A in energy. Thus, isomer 9A is the most probable structure observed in our experiments.

2.2.9. $CoGe_{10}^-$

DFT calculations by Li et al. suggested that the most stable structure of $CoGe_{10}^-$ was a D_{4d} bicapped tetragonal antiprism, and the second most stable structure was a C_{3v} tetracapped trigonal prism, which was higher in energy than the D_{4d} structure by only 2.7 kcal mol^{-1}.[3] Uta et al. predicted a singlet C_{3v} polyhedral structure for $Co@Ge_{10}^-$.[25] Herein, we have considered many initial structures for the $CoGe_{10}^-$ cluster, including those reported previously. We found the most stable isomer of the $CoGe_{10}^-$ cluster (10A; Figure 2) formed by the addition of two germanium atoms over the boat-shaped structure of $CoGe_8^-$ (isomer 8A). Thus, the cobalt atom is fully encapsulated inside the Ge_{10} cage. Isomer 10A was named a 1-5-4 layered structure by Jing et al.[12] and Kapila et al.[19] It can also be viewed as a cobalt atom at the center of a Ge_8 tetragonal prism with the other two germanium atoms capping the tetragonal prism from two neighboring side faces.

The theoretical VDE of 10A (3.35 eV; Table 2) is in reasonable agreement with the experimental value (3.63 eV). Isomers 10B and 10C are also endohedral structures. Isomer 10B is a bicapped tetragonal antiprism, similar to the most stable structure reported by Li et al.,[3] but with lower symmetry. It is much less stable than 10A by 0.53 eV in energy, and its calculated VDE (2.89 eV) is much lower than the experimental value. Isomer 10C is less stable than 10A by 1.12 eV in energy, and its calculated VDE (3.00 eV) is also much lower than the experimental value. Therefore, we suggest that isomer 10A is the most probable structure detected in our experiments. The most stable structure found by us was different from that reported by Li et al.[3] and Uta et al.[25] This is probably because we used a larger basis set in this study.

2.2.10. $CoGe_{11}^-$

The most stable isomer of $CoGe_{11}^-$ cluster (11A; Figure 2) is an endohedral structure, which can be viewed as a basket-shaped structure with two germanium atoms forming the handle of the basket, the other germanium atoms forming the container part of the basket, with the cobalt atom encapsulated inside the basket. Isomer 11A was named a 1-4-4-2 layered structure by Jing et al.[12] and Kapila et al.[19] The second most stable isomer (11B) can be described as a germanium atom capping a $CoGe_{10}$ pentagonal prism with the cobalt atom at the center; its energy is only 0.17 eV higher than that of 11A. The theoretical VDEs of 11A (3.27 eV) and 11B (3.18 eV) are in agreement with the experimental value (3.38 eV). Isomer 11C is also an endohedral structure. It is higher in energy than isomer 11A by 0.27 eV, and its calculated VDE (3.00 eV) is much lower than the experimental value. Thus, it is unlikely for isomer 11C to be present in the experiments. We suggest that isomer 11A is the

most probable one observed in our experiments and isomer 11B may also exist.

After investigation of the structures of the $CoGe_n^-$ ($n=2$–11) cluster anion, we also investigated the structures of neutral $CoGe_n$ ($n=2$–11) clusters; these are presented in Figure 3. The most stable structures of the neutral $CoGe_n$ clusters are very similar to those of the $CoGe_n^-$ anions, except that the structures of $CoGe_6$ and $CoGe_{11}$ are slightly different from those of their anionic counterparts. The lowest energy structure of neutral $CoGe_6$ (6A′; Figure 3) is a germanium-capped $CoGe_5$ square bipyramid, whereas that of the $CoGe_6^-$ anion (6A; Figure 2) is a pentagonal bipyramid with the cobalt atom at the vertex. The other two low-energy structures of neutral $CoGe_6$ are pentagonal bipyramids with the cobalt atom at the equatorial ring (6B′) and the vertex (6C′), respectively. The most stable structure of neutral $CoGe_6$ found herein is similar to that reported by Jing et al.,[12] whereas the second most stable structure of neutral $CoGe_6$ is similar to that reported by Kapila et al.[19] For $CoGe_{11}$, the most stable structure (11A′) can be considered as a germanium atom capping the most stable structure of $CoGe_{10}$ (isomer 10A′), which is slightly different from the 1-4-4-2 layered structure reported by Jing et al.[12] and Kapila et al.[19] The second most stable isomer (11B′) is similar to the most stable structure of the $CoGe_{11}^-$ anion (11A, basket-shaped structure), and it is higher in energy than 11A′ by only 0.10 eV.

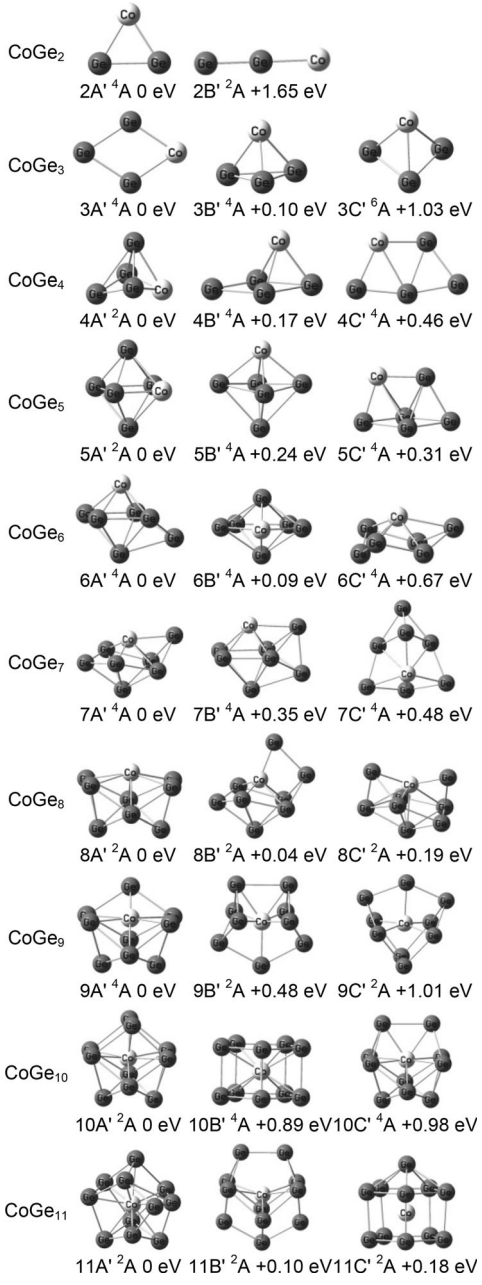

Figure 3. Optimized geometries of the low-lying isomers of $CoGe_n$ ($n=2$–11) clusters. The relative energies to the most stable isomers are shown.

3. Discussion

Overall, the most stable structures of the small anionic and neutral $CoGe_n$ clusters, with $n=2$–6, can be considered as a cobalt atom substituting one of the germanium atoms in the corresponding Ge_{n+1} clusters, which are similar to the structures of the small $TiGe_n^-$ clusters that we investigated previously.[38] The dominant structures of the $CoGe_n^{-/0}$ clusters detected in our experiments are exohedral structures for clusters with $n\leq 7$. At $n=8$, the cobalt atom is half-encapsulated by a boat-shaped Ge_8 framework, and the cobalt atom is encapsulated into the Ge_n cage at $n=9$–11.

We conducted natural population analysis (NPA) on the anionic and neutral $CoGe_n$ clusters to provide detailed information about the electronic properties of these clusters. The charges on the cobalt atom for the most stable isomers of anionic and neutral $CoGe_n$ clusters are shown in Table 3. As observed from the results in Table 3, the negative charge is mainly localized on the Ge atoms for the small $CoGe_n^-$ clusters, with $n=2$–6, and then there is slight electron transfer from the Ge_n framework to the Co atom at $n=7$ and 8. For larger clusters, such as $CoGe_9^-$, $CoGe_{10}^-$, and $CoGe_{11}^-$, the negative charge on the Co atom increases significantly, and electron transfer from the Ge atoms to the Co atom is much more than that in $CoGe_7^-$ and $CoGe_8^-$. Similar to the case of anionic clusters, in the neutral $CoGe_n$ clusters, the Ge_n framework is negatively charged for cluster sizes with $n=2$–6, whereas for a cluster size with $n=7$–11, there is electron transfer from the Ge atoms to the Co atom and the Co atom is negatively charged. This indicates that electron transfer from the Ge_n framework to the Co atom is strongly related to the structural evolution of $CoGe_n$ clusters, especially related to the formation of endohedral structures. The natural electron configurations show that the electrons are distributed on the 3d, 4s, and 4p orbitals of the Co atom, and the 4s orbital loses some of its electrons, while the empty 4p orbitals gain electrons; this indicates that there are strong spd hybridizations for the Co atom in both anionic and neutral $CoGe_n$ clusters, especially for clusters with $n=9$–11. This is in agreement with studies on neutral $CoGe_n$ clusters conducted by Jing et al.[12] and Kapila et al.[19] as well as that of WGe_n clusters by Wang and Han.[7]

Herein, we consider the magnetic properties of $CoGe_n^{-/0}$ ($n=2$–11) clusters. As displayed in Table 3, for the anions, the total magnetic moments are 2 μ_B for cluster sizes of $n=2$–9,

Table 3. NPA charges, atomic magnetic moments (μ_A), total magnetic moments (μ_T), and natural electron configuration of the most stable isomers of $CoGe_n^-$ ($n=2$–11) and $CoGe_n$ ($n=2$–11) clusters.

Cluster	NPA charge on Co [e]	μ_T [μ_B]	μ_{Co} [μ_B]	Natural electron configuration on Co
$CoGe_2^-$	−0.02	2	2.08	$3d^{7.99}4s^{0.76}4p^{0.24}4d^{0.01}$
$CoGe_3^-$	0.01	2	2.08	$3d^{8.00}4s^{0.73}4p^{0.26}$
$CoGe_4^-$	−0.07	2	2.00	$3d^{8.03}4s^{0.60}4p^{0.41}4d^{0.02}$
$CoGe_5^-$	−0.01	2	2.08	$3d^{7.95}4s^{0.60}4p^{0.44}4d^{0.01}$
$CoGe_6^-$	−0.20	2	1.99	$3d^{8.05}4s^{0.57}4p^{0.54}4d^{0.02}$
$CoGe_7^-$	−0.61	2	1.92	$3d^{8.17}4s^{0.52}4p^{0.87}4d^{0.04}$
$CoGe_8^-$	−0.42	2	1.99	$3d^{8.06}4s^{0.53}4p^{0.77}4d^{0.04}$
$CoGe_9^-$	−1.81	2	1.67	$3d^{8.54}4s^{0.51}4p^{1.57}4d^{0.17}$
$CoGe_{10}^-$	−3.11	0	0	$3d^{9.49}4s^{0.40}4p^{1.98}4d^{0.23}$
$CoGe_{11}^-$	−2.29	0	0	$3d^{9.32}4s^{0.38}4p^{1.45}4d^{0.10}$
$CoGe_2$	0.16	3	2.18	$3d^{7.93}4s^{0.72}4p^{0.17}4d^{0.01}$
$CoGe_3$	0.38	3	2.37	$3d^{7.73}4s^{0.72}4p^{0.17}4d^{0.01}$
$CoGe_4$	0.14	1	1.84	$3d^{8.01}4s^{0.52}4p^{0.30}4d^{0.02}$
$CoGe_5$	0.06	1	2.12	$3d^{7.93}4s^{0.58}4p^{0.40}4d^{0.01}$
$CoGe_6$	0.28	1	1.92	$3d^{7.92}4s^{0.61}4p^{0.39}4d^{0.01}$
$CoGe_7$	−0.50	3	2.19	$3d^{8.11}4s^{0.53}4p^{0.81}4d^{0.04}$
$CoGe_8$	−0.38	1	1.95	$3d^{8.08}4s^{0.54}4p^{0.70}4d^{0.04}$
$CoGe_9$	−1.58	3	1.95	$3d^{8.51}4s^{0.51}4p^{1.40}4d^{0.14}$
$CoGe_{10}$	−2.96	1	1.04	$3d^{9.11}4s^{0.45}4p^{2.10}4d^{0.28}$
$CoGe_{11}$	−2.96	1	0.73	$3d^{9.29}4s^{0.43}4p^{1.97}4d^{0.27}$

and 0 μ_B for cluster sizes of $n=10$ and 11. For the neutral $CoGe_n$ clusters, the total magnetic moments are 3 μ_B for $n=2$, 3, 7, and 9, and 1 μ_B for $n=4$, 5, 6, 8, 10, and 11. For both anionic and neutral $CoGe_n$ clusters, the magnetic moments decreased to the lowest values at $n=10$ and 11, and this tendency is in agreement with previous DFT calculations on $CoGe_n$[12,19] and the investigation into Si_nCo ($n=10$–12) clusters conducted by Li et al.[39] The minimization of the magnetic moments at $n=10$ and 11 is also in agreement with the formation of endohedral structures in $CoGe_n$ clusters and is consistent with the results for the $CrSi_n^-$ ($n=3$–12) clusters reported by Kong et al.[40] From Table 3, we can see that the total magnetic moments are mainly contributed to by the cobalt atom because the local magnetic moments on the cobalt atom are close to the total magnetic moments in general. The minimization of the magnetic moments for these clusters can be ascribed to charge transfer from the germanium atoms to cobalt atom and strong *spd* hybridizations of the cobalt atom. For $CoGe_n$ with $n=4$–6, and 8, the total magnetic moments are slightly smaller than the local magnetic moments on the cobalt atom because some local moments of the germanium atoms align antiferromagnetically to that of the cobalt atom.[12,19]

4. Conclusions

The geometrical structures and electronic and magnetic properties of $CoGe_n^{-/0}$ ($n=2$–11) clusters were investigated by using anion photoelectron spectroscopy and DFT calculations. The critical size of the transition from exo- to endohedral structures was $n=9$. The NPA showed that the negative charges transferred from the Ge_n framework to the Co atom for both anionic and neutral $CoGe_n$ clusters with $n\geq 7$. The total magnetic moments of anionic and neutral $CoGe_n$ clusters were mainly contributed to by the local magnetic moments of the Co atom, and the magnetic moments decreased to the lowest value at $n=10$ and 11. For both anionic and neutral $CoGe_n$ clusters, there were strong *spd* hybridizations for the Co atom, especially for the clusters with $n=9$–11. The NPA charge distributions and the change in the magnetic moments were related to structural evolution.

Experimental Section

The experiments were conducted on a homemade apparatus equipped with a laser vaporization cluster source, a time-of-flight mass spectrometer, and a magnetic-bottle photoelectron spectrometer, as described elsewhere.[41] The $CoGe_n^-$ ($n=2$–11) cluster anions were generated in the laser vaporization source by laser ablation of a rotating translating disk target (13 mm diameter; Co/Ge molar ratio of 1:4) with the second harmonic of a nanosecond Nd:YAG laser (Continuum Surelite II-10). Helium gas with about 4 atm back pressure was allowed to expand through a pulsed valve (General Valve Series 9) into the source to cool the formed clusters. The generated cluster anions were mass-analyzed with the time-of-flight mass spectrometer. The cluster anions of interest were selected with a mass gate, decelerated by a momentum decelerator, and crossed with the beam of another Nd:YAG laser (Continuum Surelite II-10, 266 nm) at the photodetachment region. The electrons from photodetachment were energy-analyzed by the magnetic-bottle photoelectron spectrometer. The photoelectron spectra were calibrated with the spectra of Cu^- and Pb^- recorded under similar conditions. The resolution of the magnetic-bottle photoelectron spectrometer was about 40 meV at an electron kinetic energy of 1 eV.

Geometry optimizations of $CoGe_n^{-/0}$ ($n=2$–11) clusters were performed by using DFT with the spin-unrestricted B3PW91 exchange-correlation functional[42–45] and 6-311+G(d) basis sets, as implemented in the Gaussian 09 package.[46] For all clusters, many initial structures were constructed by Co substitution or Co capping of pure Ge_n clusters, or based on the structures of TM-doped Ge_n clusters reported in the literature.[6–8,10,13,15,21,26] All geometries were optimized without any symmetry constraints. Harmonic vibrational frequencies were calculated to make sure that the structures corresponded to real local minima, and the zero-point vibrational energy corrections were included for the relative energies of isomers. The charges and magnetic moments were evaluated by NPA by using the natural bond orbital (NBO) version 3.1 program[47–54] implemented in the Gaussian 09 package.[46]

Acknowledgements

W.-J.Z. acknowledges the Knowledge Innovation Program of the Chinese Academy of Sciences (grant no. KJCX2-EW-H01) and H.-G. X. acknowledges the National Natural Science Foundation of China (grant no. 21103202) for financial support. The theoretical calculations were conducted on the ScGrid and DeepComp 7000 of the Supercomputing Center, Computer Network Information Center of the Chinese Academy of Sciences.

Keywords: density functional calculations · cluster compounds · magnetic properties · photoelectron spectroscopy · semiconductors

[1] Y. Kamata, *Mater. Today* **2008**, *11*, 30 – 38.
[2] R. Pillarisetty, *Nature* **2011**, *479*, 324 – 328.
[3] G. L. Li, X. Zhang, Z. C. Tang, Z. Gao, *Chem. Phys. Lett.* **2002**, *359*, 203 – 212.
[4] V. Kumar, Y. Kawazoe, *Phys. Rev. Lett.* **2002**, *88*, 235504.
[5] V. Kumar, A. K. Singh, Y. Kawazoe, *Nano Lett.* **2004**, *4*, 677 – 681.
[6] J. Wang, J. G. Han, *J. Chem. Phys.* **2005**, *123*, 244303.
[7] J. Wang, J.-G. Han, *J. Phys. Chem. A* **2006**, *110*, 12670 – 12677.
[8] J. Wang, J.-G. Han, *J. Phys. Chem. B* **2006**, *110*, 7820 – 7827.
[9] X. J. Hou, G. Gopakumar, P. Lievens, M. T. Nguyen, *J. Phys. Chem. A* **2007**, *111*, 13544 – 13553.
[10] J. Wang, J.-G. Han, *Chem. Phys.* **2007**, *342*, 253 – 259.
[11] W.-J. Zhao, Y.-X. Wang, *Chem. Phys.* **2008**, *352*, 291 – 296.
[12] Q. Jing, F. Y. Tian, Y. X. Wang, *J. Chem. Phys.* **2008**, *128*, 124319.
[13] X. J. Li, K. H. Su, *Theor. Chem. Acc.* **2009**, *124*, 345 – 354.
[14] V. T. Ngan, J. De Haeck, H. T. Le, G. Gopakumar, P. Lievens, M. T. Nguyen, *J. Phys. Chem. A* **2009**, *113*, 9080 – 9091.
[15] W.-J. Zhao, Y.-X. Wang, *J. Mol. Struct. THEOCHEM* **2009**, *901*, 18 – 23.
[16] D. Bandyopadhyay, P. Kaur, P. Sen, *J. Phys. Chem. A* **2010**, *114*, 12986 – 12991.
[17] D. Bandyopadhyay, P. Sen, *J. Phys. Chem. A* **2010**, *114*, 1835 – 1842.
[18] C. Tang, M. Liu, W. Zhu, K. Deng, *Comput. Theor. Chem.* **2011**, *969*, 56 – 60.
[19] N. Kapila, V. K. Jindal, H. Sharma, *Phys. B* **2011**, *406*, 4612 – 4619.
[20] D. Bandyopadhyay, *J. Mol. Model.* **2012**, *18*, 3887 – 3902.
[21] M. Kumar, N. Bhattacharyya, D. Bandyopadhyay, *J. Mol. Model.* **2012**, *18*, 405 – 418.
[22] G. Gopakumar, P. Lievens, M. T. Nguyen, *J. Chem. Phys.* **2006**, *124*, 214312.
[23] G. Gopakumar, P. Lievens, M. T. Nguyen, *J. Phys. Chem. A* **2007**, *111*, 4353 – 4361.
[24] G. Gopakumar, X. Wang, L. Lin, J. De Haeck, P. Lievens, M. T. Nguyen, *J. Phys. Chem. C* **2009**, *113*, 10858 – 10867.
[25] M. M. Uţă, D. Cioloboc, R. B. King, *Inorg. Chem.* **2012**, *51*, 3498 – 3504.
[26] K. Dhaka, R. Trivedi, D. Bandyopadhyay, *J. Mol. Model.* **2013**, *19*, 1473 – 1488.
[27] X. Zhang, G. L. Li, Z. Gao, *Rapid Commun. Mass Spectrom.* **2001**, *15*, 1573 – 1576.
[28] J. Atobe, K. Koyasu, S. Furuse, A. Nakajima, *Phys. Chem. Chem. Phys.* **2012**, *14*, 9403 – 9410.
[29] S. Furuse, K. Koyasu, J. Atobe, A. Nakajima, *J. Chem. Phys.* **2008**, *129*, 064311.
[30] X. J. Li, K. H. Su, X. H. Yang, L. M. Song, L. M. Yang, *Comput. Theor. Chem.* **2013**, *1010*, 32 – 37.
[31] C. Krontiras, S. N. Georga, S. Sakkopoulos, E. Vitoratos, J. Salmi, *J. Phys. Condens. Matter* **1990**, *2*, 3323 – 3328.
[32] Y. J. Cho, C. H. Kim, H. S. Kim, W. S. Lee, S.-H. Park, J. Park, S. Y. Bae, B. Kim, H. Lee, J.-Y. Kim, *Chem. Mater.* **2008**, *20*, 4694 – 4702.
[33] K. Park, C. H. An, M. S. Lee, C. W. Yang, H. J. Lee, H. Kim, *J. Electrochem. Soc.* **2009**, *156*, H229 – H232.
[34] H. Yoon, K. Seo, N. Bagkar, J. In, J. Park, J. Kim, B. Kim, *Adv. Mater.* **2009**, *21*, 4979 – 4982.
[35] K. De Keyser, R. L. Van Meirhaeghe, C. Detavernier, J. Jordan-Sweet, C. Lavoie, *J. Electrochem. Soc.* **2010**, *157*, H395 – H404.
[36] H. Yoon, S.-i. Kim, S. Lee, J. In, J. Kim, H. Ryoo, J.-H. Noh, J.-P. Ahn, Y. Jo, J. Choo, B. Kim, *J. Mater. Chem. C* **2013**, *1*, 6259 – 6264.
[37] J. Q. Wang, S. Stegmaier, T. F. Fassler, *Angew. Chem. Int. Ed.* **2009**, *48*, 1998 – 2002; *Angew. Chem.* **2009**, *121*, 2032 – 2036.
[38] X.-J. Deng, X.-Y. Kong, X.-L. Xu, H.-G. Xu, W.-J. Zheng, *RSC Adv.* **2014**, *4*, 25963 – 25968.
[39] Y. Li, N. M. Tam, P. Claes, A. P. Woodham, J. T. Lyon, V. T. Ngan, M. T. Nguyen, P. Lievens, A. Fielicke, E. Janssens, *J. Phys. Chem. A* **2014**, *118*, 8198 – 8203.
[40] X. Y. Kong, H. G. Xu, W. J. Zheng, *J. Chem. Phys.* **2012**, *137*, 064307.
[41] H. G. Xu, Z. G. Zhang, Y. Feng, J. Y. Yuan, Y. C. Zhao, W. J. Zheng, *Chem. Phys. Lett.* **2010**, *487*, 204 – 208.
[42] J. P. Perdew, J. A. Chevary, S. H. Vosko, K. A. Jackson, M. R. Pederson, D. J. Singh, C. Fiolhais, *Phys. Rev. B* **1992**, *46*, 6671 – 6687.
[43] J. P. Perdew, J. A. Chevary, S. H. Vosko, K. A. Jackson, M. R. Pederson, D. J. Singh, C. Fiolhais, *Phys. Rev. B* **1993**, *48*, 4978 – 4978.
[44] A. D. Becke, *J. Chem. Phys.* **1993**, *98*, 5648 – 5652.
[45] J. P. Perdew, K. Burke, Y. Wang, *Phys. Rev. B* **1996**, *54*, 16533 – 16539.
[46] Gaussian 09, Revision C.01, M. J. Frisch, G. W. Trucks, H. B. Schlegel, G. E. Scuseria, M. A. Robb, J. R. Cheeseman, G. Scalmani, V. Barone, B. Mennucci, G. A. Petersson, H. Nakatsuji, M. Caricato, X. Li, H. P. Hratchian, A. F. Izmaylov, J. Bloino, G. Zheng, J. L. Sonnenberg, M. Hada, M. Ehara, K. Toyota, R. Fukuda, J. Hasegawa, M. Ishida, T. Nakajima, Y. Honda, O. Kitao, H. Nakai, T. Vreven, J. A. Montgomery, Jr., J. E. Peralta, F. Ogliaro, M. Bearpark, J. J. Heyd, E. Brothers, K. N. Kudin, V. N. Staroverov, R. Kobayashi, J. Normand, K. Raghavachari, A. Rendell, J. C. Burant, S. S. Iyengar, J. Tomasi, M. Cossi, N. Rega, J. M. Millam, M. Klene, J. E. Knox, J. B. Cross, V. Bakken, C. Adamo, J. Jaramillo, R. Gomperts, R. E. Stratmann, O. Yazyev, A. J. Austin, R. Cammi, C. Pomelli, J. W. Ochterski, R. L. Martin, K. Morokuma, V. G. Zakrzewski, G. A. Voth, P. Salvador, J. J. Dannenberg, S. Dapprich, A. D. Daniels, Ö. Farkas, J. B. Foresman, J. V. Ortiz, J. Cioslowski, D. J. Fox, Gaussian, Inc., Wallingford CT, **2009**.
[47] J. P. Foster, F. Weinhold, *J. Am. Chem. Soc.* **1980**, *102*, 7211 – 7218.
[48] A. E. Reed, F. Weinhold, *J. Chem. Phys.* **1983**, *78*, 4066 – 4073.
[49] A. E. Reed, F. Weinhold, *J. Chem. Phys.* **1985**, *83*, 1736 – 1740.
[50] A. E. Reed, R. B. Weinstock, F. Weinhold, *J. Chem. Phys.* **1985**, *83*, 735 – 746.
[51] J. E. Carpenter, University of Wisconsin, Madison, **1987**.
[52] A. E. Reed, L. A. Curtiss, F. Weinhold, *Chem. Rev.* **1988**, *88*, 899 – 926.
[53] F. Weinhold, J. E. Carpenter in *The Structure of Small Molecules and Ions* (Eds.: R. Naaman, Z. Vager), Plenum, New York, **1988**, p. 227.
[54] J. E. Carpenter, F. Weinhold, *J. Mol. Struct. THEOCHEM* **1988**, *169*, 41 – 62.

Received: September 4, 2014
Published online on October 7, 2014